

JANUSZ CYGANKIEWICZ\*, JÓZEF KNECHTEL\*

**THE EFFECT OF TEMPERATURE OF ROCKS ON MICROCLIMATIC CONDITIONS  
IN LONG GATE ROADS AND GALLERIES IN COAL MINES****WPLYW TEMPERATURY PIERWOTNEJ SKAŁ NA PARAMETRY MIKROKLIMATU  
W DŁUGICH WYROBISKACH KORYTARZOWYCH**

The aim of this study was to examine the effect of the temperature of surrounding rocks on enthalpy and temperature of air flowing along several model mine workings. Long workings surrounded by non-coal rocks as well longwall gates surrounded by coal were taken into consideration. Computer-aided simulation methods were used during the study. At greater depths the amount of moisture transferred into a mine working from the rock mass is two orders of magnitude smaller than the moisture that comes from external (technological) sources, mainly from coal extraction-related processes, therefore in the equation describing temperature changes only the terms representing the flux of heat from rocks were included. The model workings, for calculation purposes, were divided into sections, 50 m in length each. For each of the sections temperature of its ribs and temperature and stream of enthalpy of air flowing along it were calculated with the use of the finite differences method. For workings surrounded by non-coal rocks two variant calculations were carried out, namely with or without technological sources of heat. For coal surrounded workings (longwall gates) a new method for determination of heat from coal oxidation was developed, based on the findings by Cygankiewicz J. (2012a, 2012b). Using the results of a study by J.J. Drzewiecki and Smolka (1994), the effects of rock mass fracturing on transfer of heat into the air stream flowing along a working were taken into account.

**Keywords:** safety, ventilation, air-conditioning, heat and mass transfer

Badano wpływ temperatury pierwotnej skał na strumień entalpii oraz temperaturę powietrza w wyrobisku korytarzowym o długości 2000 m. Rozpatrywano wyrobiska kamienne oraz chodniki podścianowe. W badaniach zastosowano metodę symulacji komputerowych. Na dużych głębokościach wilgoć przenoszona z górotworu do wyrobiska jest dwa rzędy wielkości mniejsza od wilgoci pochodzącej od procesów technologicznych. W związku z powyższym w równaniu opisującym zmiany temperatury w masywie skalnym uwzględniono tylko człon reprezentujący ruch ciepła w skałach. Badane wyrobisko podzielono na odcinki o długości 50 m. Korzystając z metody różnic skończonych dla każdego z odcinków wyznaczono temperaturę ociosu, a następnie temperaturę i strumień entalpii powietrza. W odniesieniu do wyrobisk kamiennych rozważania przeprowadzono dla wariantu z technologicznymi źródłami ciepła oraz

\* CENTRAL MINING INSTITUTE, PL. GWARKÓW 1, 40-166 KATOWICE, POLAND

bez takich źródeł. Dla chodników węglowych przedstawiono nowy sposób określenia ciepła utleniania węgla, na podstawie wyników badań J. Cygankiewicza (2012a, 2012b). Korzystając z wyników badań J. Drzewieckiego i J. Smolki (1994), uwzględniono wpływ spekań górotworu na przenoszenie ciepła do powietrza w wyrobisku.

**Słowa kluczowe:** bezpieczeństwo, aerologia, klimatyzacja, przepływ ciepła i masy

## 1. Introduction

In our former studies pertaining to exchange of heat between the rock mass and the air stream flowing along a mine working the assumed maximal temperature of surrounding rocks was 40°C and the maximal length of workings (longwall gates) was 1,000 m. Also, we assumed the value of about 12 m<sup>2</sup> for the cross section of a typical mine working, that limited the airflow volume possible to convey through such a working. These previously assumed values now are becoming outdated. The modern mining requires high concentration of coal extraction, therefore the technology-related heat sources became the main cause of occupational climate problems. Nowadays, in Polish and Czech coal mines, the virgin temperature of rock mass reaches 50°C whereas the length of auxiliary ventilated working nears 4000 meters. The cross sections area of a gate often exceeds 20 m<sup>2</sup>, thus enabling us, by means of optimization of mine ventilation networks, to increase the intensity of ventilation of underground workings.

The aim of this study is to examine the effect of rock mass temperature on enthalpy of air flowing along such mine workings. In the planning stage of mining operations one has to take into account two adverse phenomena, namely, that the heat flux coming from rock mass having temperature 50°C will be nearly two times higher than one from rocks of 40°C in temperature and the “buffering effect” of rock mass on heat flux coming from technological sources of heat will be very small.

## 2. The method of calculations

Mine workings ventilated by means of flow-through ventilation are considered here. The model applied in this work has been positively verified for the conditions of Polish mines of the Upper Silesia Coal Basin and Czech Coal Company OKD. In our study a computer-aided simulation method was used. The survey of the status of climate – related occupational hazard in Polish coal mines for the year 2011 showed that the cross-sectional area of longwall gates ranged from 8 to 17.8 m<sup>2</sup> (12.86 m<sup>2</sup> on average), therefore, in our study, the value  $A = 13,5 \text{ m}^2$  was assumed. Calculations were carried out also for three arbitrarily assumed values of virgin temperature of rock mass, namely:  $t_{pg1} = 35^\circ\text{C}$ ,  $t_{pg2} = 40^\circ\text{C}$  and  $t_{pg3} = 50^\circ\text{C}$ . It was assumed also that the typical length of gate is 2000 m and the velocity of air flow is 1 m/s. Taking advantage of the results of underground measurements and empirical studies on moisture stream increase along longwalls and longwall gates, carried out in selected mines by the author (Knechtel, 2009) it was assumed that the moisture stream coming from coal-extraction related processes (technological sources) was  $9.33 \cdot 10^{-2} \text{ kg/s}$ . It was assumed also that the total power of coal extraction equipment acting along a gate is about 1 MW, and those power sources are distributed evenly along the gate.

The studies on spatial distribution of virgin temperature of rock mass, carried out in the Central Institute of Mining (Knechtel & Gapinski, 2005) showed that the geothermal gradient

when calculated for the distance between two deep mining levels differs significantly from the gradient calculated between the surface of the mine and a particular mining level, usually the latter is below 25 m/K. That is why it was assumed in this paper that virgin temperature of rock mass reaches 35°C at 780 m level, 40°C at 890 m level and 50°C at 1115 m level. The assumed atmospheric pressure at these levels is respectively: at 780 m – 110700 Pa, at 890 m – 112000 Pa and at 1115 m – 114700Pa.

For these assumptions several micro-climate-related parameters of flowing air were calculated for each of 50-meter long sections of a working (longwall gate). Calculations were carried out for the three above mentioned values of virgin rock mass temperature and for two situation variants: namely with and without heat and moisture coming from technological sources. Since the flow of heat and moisture coming from the rock mass into air stream flowing along a working depends, among others, on the difference between temperature of ribs  $t_s$  and temperature of air stream  $t_w$ , for each of the sections of the working the value of temperature of ribs had to be determined. Because the duration of ventilation period for each section of the gate and the temperature of air flowing along such a section are usually different, therefore different are also the values of heat flux coming from rocks surrounding the working.

The temperature ( $t_g$ ) and humidity ( $\omega_g$ ) fields across rock mass can be represented in the form of the following system of equations (Knechtel, 1998a):

$$\begin{aligned} \frac{\partial t_g(s, \tau)}{\partial \tau} &= A \left[ \frac{\partial^2 t_g(s, \tau)}{\partial s^2} + \frac{1}{s} \frac{\partial t_g(s, \tau)}{\partial s} \right] + B \left[ \frac{\partial^2 \omega_g(s, \tau)}{\partial s^2} + \frac{1}{s} \frac{\partial \omega_g(s, \tau)}{\partial s} \right] \\ \frac{\partial \omega_g(s, \tau)}{\partial \tau} &= C \left[ \frac{\partial^2 t_g(s, \tau)}{\partial s^2} + \frac{1}{s} \frac{\partial t_g(s, \tau)}{\partial s} \right] + D \left[ \frac{\partial^2 \omega_g(s, \tau)}{\partial s^2} + \frac{1}{s} \frac{\partial \omega_g(s, \tau)}{\partial s} \right] \end{aligned} \quad (1)$$

whereas the boundary conditions are:

$$\lambda_q \frac{dt_g}{ds} \Big|_{s=r_w} = q_w \quad (2)$$

$$\lambda_h \frac{d\omega_g}{ds} \Big|_{s=r_w} = j_w \quad (3)$$

$$t_g(\infty, \tau) = t_{pg} \quad (4)$$

$$\omega_g(\infty, \tau) = \omega_{pg} \quad (5)$$

and the initial conditions are specified by the following equations:

$$t_g(s, 0) = t_{pg} \quad (6)$$

$$\omega_g(s, 0) = \omega_{pg} \quad (7)$$

The coefficients  $A, B, C, D$  in the equations (1) are defined by the following formulas:

$$A = a_q + \varepsilon a' a_h c_w \delta / c_q \quad (8)$$

$$B = \varepsilon a' a_h c_w / c_q \quad (9)$$

$$C = a_h \delta \quad (10)$$

$$D = a_h \quad (11)$$

where:

- $q_w$  — density of heat flux from rock mass, W/m<sup>2</sup>;
- $j_w$  — density of moisture flux from rock mass, kg/(m<sup>2</sup>·s);
- $t_{pg}$  — virgin temperature of rock mass, °C;
- $\omega_{pg}$  — moisture movement potential for initial state ( after Holek, 1990), J/kmol;
- $a_q$  — coefficient of balancing of temperature of rocks mass, m<sup>2</sup>/s;
- $a_h$  — coefficient of balancing of moisture of rocks mass (after Holek, 1979), m<sup>2</sup>/s;
- $c_q$  — specific heat capacity of rocks mass, J/(kg K);
- $c_w$  — specific isothermal moisture capacity of rock mass (after Holek, 1979), kmol/J;
- $e$  — coefficient of moisture phase transformation (after Holek, 1990);
- $l_q$  — coefficient of thermal conductivity of rock mass, W/(m K);
- $l_h$  — thermal conductivity of moisture in the rock mass (after S. Holek 1979), kg/(m s J/kmol).

Sidiropoulos and Tzimopoulos (1983) found that the interaction between the fields of potential of heat and moisture movement is low, therefore the fields of temperature and moisture within the rock mass can be considered separately. Solutions were found with the use of Laplace integral transformation. Similar results are obtained using the method of finite differences, where derivatives are replaced by differences (Nikitenko, 1971):

$$\frac{\partial t}{\partial \tau} \approx \frac{t_j^{n+1} - t_j^n}{l} \quad (12)$$

$$\frac{\partial t}{\partial s} = \frac{t_{j+1}^n - t_{j-1}^n}{2h} \quad (13)$$

$$\frac{\partial^2 t}{\partial s^2} = \frac{t_{j+1}^n + t_{j-1}^n - 2t_j^n}{h^2} \quad (14)$$

where:

- $l$  — time interval, s;
- $h$  — spatial section (thickness of seam or layer), m;
- $t_j^n$  — temperature of rock at 'n' moment along 'j' spatial section, °C.

Then the first of the equations (1) can be written as:

$$t_j^{n+1} = t_j^n + \frac{l \cdot a_q}{h^2} \left[ (t_{j+1}^n + t_{j-1}^n - 2t_j^n) + \frac{h}{2r_j} (t_{j+1}^n - t_{j-1}^n) \right] \quad (15)$$

where:  $r_j = r_w + h(j-1)$ ;  $r_w$  — radius of the gate, m and  $n = 0, 1, 2, 3, j = 1, 2, 3$ , for  $n = 0$   $t = t_{pg}$  and for  $j \rightarrow \infty$   $t = t_{pg}$ , while boundary condition for the initial moment can be

written as:

$$\lambda_q \frac{t_{pg} - t_s}{h} = \alpha (t_s - t_0) \quad (16)$$

where:

- $t_s$  — temperature of ribs of the gate, °C;
- $t_0$  — temperature of air stream in the gate, °C;
- $\alpha$  — coefficient of heat transfer from the walls of the gate, W/(m<sup>2</sup>·K).

Analogous reasoning has been carried out for the potential of moisture movement within rock mass  $\omega g$ . In this study we modified the coefficients of moisture movement developed by S. Holec (1979, 1990). It should be noted that, while the heat fluxes coming from coal extraction machines and from rock mass are closely comparable, the moisture flux from rock mass is an order of magnitude smaller than the moisture that comes from technological sources.

The value of air temperature for each of gate sections was calculated using the formula (Knechtel, 1998b):

$$t_w = t_d + \frac{\alpha}{m \cdot c_p} B (t_s - t_d) + \frac{Q_z}{m \cdot c_p} \quad (17)$$

where:

- $t_d$  — air temperature at the start of a 50-meter section of the gate, °C;
- $t_w$  — air temperature at the end of the gate, °C;
- $t_s$  — temperature of gate ribs, °C;
- $B$  — gate perimeter, m;
- $m$  — mass stream of air flowing along the working, kg/s;
- $Q_z$  — heat flux coming from technological sources, W;
- $\alpha$  — coefficient of heat transfer from the ribs of the gate, W/(m<sup>2</sup>·K);
- $c_p = 1006$  J/(kg·K) — specific heat capacity of air, measured at constant pressure.

In this study it was assumed that the gate (working) is horizontal. The calculations were carried out separately for gates within coal seam and ones surrounded by non-coal rock (for which the heat of oxidation of coal was omitted).

### 3. The effect of virgin temperature of rock mass on heat flux distribution along workings

#### 3.1. Computer aided simulations

Using the formulas from Chapter 2, and assuming that temperature of fresh air at the intake cross section of a gate is 20°C and its relative humidity is 72%, several variant, computer aided simulations have been carried out. The results of calculations are shown in Tables 1, 2, 3 and 4. Tables 1 and 3 refer to the variant without technological sources of heat and moisture, while Tables 2 and 4 pertain to the variant with the said sources. Tables 1 and 2 refer to changes in temperature –  $t_w$ , moisture content –  $X$  and heat flux coming from rock mass –  $q_g$ , whereas Tables 3 and 4 relate to the enthalpy of air stream along the working –  $I$ . In Tables 1 and 2, for

TABLE 1

The effect of rock mass temperature on thermal parameters of air flowing along a gate  
(no active technological heat sources)

x, m	$t_{pg} = 35^{\circ}\text{C}$			$t_{pg} = 40^{\circ}\text{C}$			$t_{pg} = 50^{\circ}\text{C}$		
	$t_w, ^{\circ}\text{C}$	$X_w, \text{kg of vapor/kg dry air}$	$q_g, \text{W/m}^2$	$t_w, ^{\circ}\text{C}$	$X_w, \text{kg of vapor/kg dry air}$	$q_g, \text{W/m}^2$	$t_w, ^{\circ}\text{C}$	$X_w, \text{kg of vapor/kg dry air}$	$q_g, \text{W/m}^2$
0	20.00	0.00961	5.646	20.00	0.00948	8.833	20.00	0.00922	13.249
50	20.25	0.00962	5.582	20.32	0.00949	8.731	20.47	0.00924	13.100
100	20.49	0.00963	5.518	20.64	0.00950	8.629	20.93	0.00925	12.957
150	20.73	0.00964	5.459	20.95	0.00951	8.535	21.39	0.00926	12.818
200	20.97	0.00965	5.394	21.26	0.00952	8.440	21.84	0.00927	12.683
250	21.21	0.00966	5.330	21.56	0.00953	8.349	22.29	0.00929	12.546
300	21.44	0.00966	5.271	21.86	0.00954	8.257	22.73	0.00930	12.412
350	21.67	0.00967	5.212	22.16	0.00955	8.164	23.17	0.00931	12.277
400	21.90	0.00968	5.153	22.45	0.00956	8.074	23.60	0.00932	12.146
450	22.12	0.00969	5.099	22.74	0.00957	7.988	24.03	0.00934	12.018
500	22.34	0.00970	5.046	23.03	0.00958	7.903	24.45	0.00935	11.899
550	22.56	0.00971	4.987	23.32	0.00959	7.817	24.87	0.00936	11.778
600	22.78	0.00971	4.933	23.60	0.00960	7.735	25.29	0.00937	11.655
650	23.00	0.00972	4.880	23.88	0.00961	7.652	25.70	0.00939	11.536
700	23.21	0.00973	4.826	24.16	0.00962	7.568	26.11	0.00940	11.415
750	23.42	0.00974	4.778	24.43	0.00963	7.492	26.51	0.00941	11.303
800	23.63	0.00975	4.724	24.70	0.00964	7.420	26.91	0.00943	11.198
850	23.84	0.00975	4.670	24.97	0.00965	7.347	27.31	0.00944	11.091
900	24.04	0.00976	4.627	25.26	0.00966	7.263	27.70	0.00945	10.988
950	24.24	0.00977	4.579	25.52	0.00966	7.192	28.09	0.00946	10.883
1000	24.44	0.00978	4.531	25.78	0.00967	7.120	28.47	0.00948	10.781
1050	24.64	0.00979	4.488	26.04	0.00968	7.055	28.85	0.00949	10.689
1100	24.84	0.00980	4.440	26.29	0.00969	6.997	29.23	0.00950	10.600
1150	25.03	0.00980	4.402	26.54	0.00970	6.937	29.60	0.00951	10.514
1200	25.22	0.00981	4.359	26.79	0.00971	6.876	29.97	0.00953	10.426
1250	25.41	0.00982	4.322	27.04	0.00972	6.814	30.34	0.00954	10.336
1300	25.60	0.00983	4.279	27.29	0.00973	6.757	30.71	0.00955	10.255
1350	25.79	0.00984	4.241	27.53	0.00974	6.709	31.07	0.00956	10.185
1400	25.98	0.00985	4.204	27.77	0.00975	6.662	31.43	0.00958	10.115
1450	26.16	0.00985	4.172	28.01	0.00976	6.620	31.79	0.00959	10.054
1500	26.34	0.00986	4.140	28.25	0.00977	6.576	32.14	0.00960	9.995
1550	26.52	0.00987	4.113	28.49	0.00978	6.540	32.49	0.00961	9.950
1600	26.70	0.00988	4.081	28.73	0.00979	6.504	32.84	0.00963	9.904
1650	26.88	0.00989	4.059	28.96	0.00980	6.481	33.19	0.00964	9.869
1700	27.06	0.00989	4.032	29.19	0.00981	6.459	33.54	0.00965	9.835
1750	27.24	0.00990	4.011	29.42	0.00982	6.448	33.89	0.00967	9.819
1800	27.42	0.00991	3.989	29.65	0.00983	6.440	34.24	0.00968	9.807
1850	27.60	0.00992	3.979	29.88	0.00984	6.448	34.58	0.00969	9.825
1900	27.78	0.00993	3.963	30.11	0.00985	6.459	34.92	0.00970	9.849
1950	27.96	0.00994	3.957	30.34	0.00986	6.492	35.27	0.00972	9.899
2000	28.14	0.00994	3.957	30.57	0.00987	6.536	35.62	0.00973	9.967

TABLE 2

The effect of rock mass temperature on thermal parameters of air flowing along a gate  
(with technological heat sources)

$x, m$	$t_{pg} = 35^{\circ}C$			$t_{pg} = 40^{\circ}C$			$t_{pg} = 50^{\circ}C$		
	$t_w, ^{\circ}C$	$X_w, kg$ of vapor/kg of dry air	$q_g, W/m^2$	$t_w, ^{\circ}C$	$X_w, kg$ of vapor/kg of dry air	$q_g, W/m^2$	$t_w, ^{\circ}C$	$X_w, kg$ of vapor/kg of dry air	$q_g, W/m^2$
0	20.00	0.00961	5.646	20.00	0.00948	8.833	20.00	0.00922	13.249
50	20.39	0.00976	5.528	20.46	0.00962	8.669	20.61	0.00937	13.038
100	20.77	0.00991	5.416	20.92	0.00977	8.504	21.21	0.00951	12.832
150	21.15	0.01005	5.298	21.37	0.00991	8.347	21.80	0.00965	12.634
200	21.52	0.01019	5.185	21.81	0.01005	8.192	22.38	0.00980	12.440
250	21.89	0.01034	5.067	22.25	0.01020	8.037	22.96	0.00994	12.243
300	22.25	0.01048	4.960	22.68	0.01034	7.883	23.53	0.01008	12.048
350	22.61	0.01063	4.847	23.11	0.01049	7.729	24.09	0.01022	11.856
400	22.96	0.01077	4.740	23.53	0.01063	7.577	24.65	0.01037	11.663
450	23.31	0.01091	4.627	23.95	0.01077	7.428	25.51	0.01051	11.333
500	23.65	0.01106	4.520	24.36	0.01092	7.284	26.05	0.01063	11.154
550	23.99	0.01120	4.413	24.77	0.01106	7.138	26.58	0.01080	10.976
600	24.32	0.01135	4.311	25.17	0.01121	6.995	27.11	0.01094	10.797
650	24.65	0.01149	4.209	25.56	0.01135	6.855	27.63	0.01108	10.619
700	24.98	0.01164	4.102	25.95	0.01149	6.713	28.14	0.01123	10.445
750	25.30	0.01178	4.000	26.33	0.01164	6.578	28.65	0.01137	10.273
800	25.62	0.01193	3.898	26.71	0.01178	6.445	29.15	0.01151	10.112
850	25.93	0.01207	3.796	27.08	0.01193	6.321	29.64	0.01165	9.952
900	26.24	0.01221	3.700	27.45	0.01207	6.184	30.13	0.01180	9.790
950	26.54	0.01236	3.598	27.81	0.01221	6.055	30.61	0.01194	9.631
1000	26.84	0.01250	3.501	28.17	0.01236	5.924	31.09	0.01208	9.469
1050	27.13	0.01265	3.410	28.52	0.01250	5.802	31.56	0.01223	9.320
1100	27.42	0.01279	3.314	28.87	0.01264	5.680	32.03	0.01237	9.171
1150	27.71	0.01294	3.217	29.22	0.01279	5.556	32.49	0.01251	9.024
1200	27.99	0.01308	3.126	29.56	0.01293	5.434	32.95	0.01266	8.875
1250	28.27	0.01323	3.030	29.90	0.01308	5.310	33.40	0.01280	8.727
1300	28.54	0.01337	2.944	30.23	0.01322	5.194	33.85	0.01294	8.586
1350	28.81	0.01351	2.853	30.56	0.01336	5.079	34.29	0.01309	8.453
1400	29.08	0.01366	2.761	30.88	0.01351	4.968	34.72	0.01323	8.323
1450	29.34	0.01380	2.670	31.20	0.01365	4.858	35.15	0.01337	8.198
1500	29.60	0.01395	2.585	31.51	0.01380	4.751	35.58	0.01351	8.070
1550	29.85	0.01409	2.499	31.82	0.01394	4.648	36.00	0.01366	7.955
1600	30.10	0.01423	2.413	32.13	0.01408	4.542	36.42	0.01378	7.838
1650	30.35	0.01438	2.322	32.43	0.01423	4.444	36.83	0.01394	7.732
1700	30.59	0.01452	2.241	32.73	0.01437	4.344	37.24	0.01409	7.624
1750	30.83	0.01467	2.156	33.03	0.01452	4.248	37.64	0.01423	7.533
1800	31.07	0.01481	2.070	33.32	0.01466	4.157	38.04	0.01437	7.442
1850	31.30	0.01495	1.989	33.61	0.01480	4.071	38.44	0.01452	7.365
1900	31.53	0.01510	1.904	33.89	0.01495	3.990	38.83	0.01466	7.295
1950	31.76	0.01524	1.823	34.17	0.01509	3.918	39.22	0.01480	7.244
2000	31.98	0.01539	1.743	34.45	0.01523	3.847	39.61	0.01494	7.201

The effect of rock mass temperature on increase of enthalpy of air flowing along a gate  
(no active technological heat sources)

$x, \text{ m}$	$t_{pg} = 35^{\circ}\text{C}$		$t_{pg} = 40^{\circ}\text{C}$		$t_{pg} = 50^{\circ}\text{C}$	
	$Q_g, \text{ kW}$	$I, \text{ kW}$	$Q_g, \text{ kW}$	$I, \text{ kW}$	$Q_g, \text{ kW}$	$I, \text{ kW}$
0	4.319	781.019	6.757	775.230	10.135	763.653
50	4.270	785.956	6.679	781.424	10.022	772.983
100	4.221	790.714	6.601	787.619	9.912	781.689
150	4.176	795.473	6.529	793.633	9.806	790.395
200	4.127	800.231	6.457	799.648	9.702	798.922
250	4.077	804.990	6.387	805.484	9.598	807.895
300	4.032	809.123	6.317	811.320	9.495	816.243
350	3.987	813.702	6.245	817.156	9.392	824.591
400	3.942	818.281	6.177	822.812	9.292	832.760
450	3.901	822.681	6.111	828.469	9.194	841.376
500	3.860	827.081	6.046	834.126	9.103	849.366
550	3.815	831.481	5.980	839.784	9.010	857.356
600	3.774	835.434	5.917	845.261	8.916	865.347
650	3.733	839.835	5.854	850.738	8.825	873.605
700	3.692	844.055	5.790	856.216	8.732	881.417
750	3.655	848.276	5.731	861.515	8.647	889.049
800	3.614	852.497	5.676	866.813	8.566	897.129
850	3.573	856.271	5.620	872.112	8.485	904.762
900	3.540	860.312	5.556	877.771	8.406	912.215
950	3.503	864.354	5.502	882.443	8.325	919.669
1000	3.466	868.395	5.447	887.563	8.247	927.392
1050	3.433	872.437	5.397	892.682	8.177	934.666
1100	3.396	876.479	5.353	897.622	8.109	941.941
1150	2.368	879.894	5.307	902.563	8.043	949.037
1200	3.335	883.757	5.260	907.503	7.976	956.581
1250	3.306	887.619	5.213	912.444	7.907	963.678
1300	3.273	891.481	5.169	917.385	7.845	970.774
1350	3.245	895.344	5.132	922.146	7.792	977.691
1400	3.216	899.207	5.096	926.907	7.738	985.057
1450	3.191	902.443	5.064	931.669	7.691	991.975
1500	3.167	906.126	5.031	936.431	7.646	998.713
1550	3.146	909.809	5.003	941.192	7.612	1005.452
1600	3.122	913.493	4.976	945.954	7.577	1012.640
1650	3.105	917.176	4.958	950.537	7.550	1019.379
1700	3.085	920.412	4.941	955.119	7.524	1026.118
1750	3.068	924.096	4.933	959.702	7.512	1033.307
1800	3.052	927.780	4.927	964.285	7.502	1040.047
1850	3.044	931.464	4.933	968.868	7.515	1046.607
1900	3.031	935.148	4.941	973.451	7.534	1053.168
1950	3.027	938.832	4.966	978.035	7.573	1060.358
2000	3.027	942.068	5.000	982.618	7.625	1067.099



TABLE 4

The effect of rock mass temperature on enthalpy increase of air flowing along a gate  
(with technological heat sources)

$x, m$	$t_{pg} = 35^{\circ}C$		$t_{pg} = 40^{\circ}C$		$t_{pg} = 50^{\circ}C$	
	$Q_g, kW$	$I, kW$	$Q_g, kW$		$Q_g, kW$	$I, kW$
0	4.319	781.019	6.757	775.230	10.135	763.653
50	4.229	794.708	6.632	789.730	9.974	781.288
100	4.143	808.221	6.506	804.679	9.816	798.304
150	4.053	821.292	6.385	819.008	9.665	815.146
200	3.967	834.187	6.267	833.161	9.517	832.260
250	3.876	847.531	6.148	847.764	9.366	848.933
300	3.794	860.252	6.030	861.745	9.217	865.432
350	3.708	873.423	5.913	876.176	9.070	881.755
400	3.626	885.971	5.796	889.985	8.922	898.531
450	3.540	898.523	5.682	903.798	8.670	920.265
500	3.458	911.344	5.572	917.882	8.533	935.531
550	3.376	923.721	5.461	931.522	8.397	952.499
600	3.298	936.369	5.351	945.433	8.260	968.309
650	3.220	948.572	5.244	958.721	8.124	983.944
700	3.138	961.226	5.135	972.012	7.990	999.852
750	3.060	973.255	5.032	985.574	7.859	1015.317
800	2.982	985.735	4.930	998.691	7.736	1030.606
850	2.904	997.590	4.836	1012.080	7.613	1045.719
900	2.830	1009.447	4.730	1025.025	7.489	1061.285
950	2.752	1021.575	4.632	1037.792	7.368	1076.227
1000	2.679	1033.257	4.532	1051.010	7.244	1091.173
1050	2.609	1045.210	4.439	1063.604	7.130	1106.392
1100	2.535	1056.718	4.345	1076.200	7.016	1121.167
1150	2.461	1068.676	4.250	1089.249	6.903	1135.765
1200	2.391	1080.008	4.157	1101.671	6.789	1150.817
1250	2.318	1091.790	4.062	1114.545	6.676	1165.243
1300	2.252	1102.947	3.973	1126.793	6.568	1179.673
1350	2.182	1114.106	3.885	1139.044	6.467	1194.376
1400	2.113	1125.715	3.801	1151.565	6.367	1208.453
1450	2.043	1136.698	3.716	1163.641	6.271	1222.533
1500	1.977	1148.132	3.635	1175.988	6.174	1236.618
1550	1.912	1158.939	3.556	1187.889	6.086	1250.976
1600	1.846	1169.748	3.475	1199.792	5.996	1263.986
1650	1.776	1181.007	3.400	1211.967	5.915	1278.621
1700	1.715	1191.640	3.323	1223.695	5.832	1292.810
1750	1.649	1202.723	3.250	1235.875	5.763	1306.371
1800	1.583	1213.359	3.180	1247.427	5.693	1319.935
1850	1.522	1223.817	3.114	1258.982	5.634	1333.954
1900	1.456	1234.726	3.052	1270.808	5.581	1347.345
1950	1.395	1245.187	2.997	1282.187	5.542	1360.739
2000	1.333	1255.919	2.943	1293.568	5.509	1374.136

the said three values of rock mass temperature the calculated values of the following parameters are presented: estimation of temperature of air at both ends of each 50 – meter long section –  $t$ , moisture content in air –  $X$ , density of heat flux from rock mass –  $q_g$ . In Table 3 and 4 the values are given of change of heat flux coming from rock mass into each segment (50 m in length) –  $Q_z$  and enthalpy of air stream –  $I$ .

Data from Tables 1 and 3 show that, regardless of the virgin temperature of rock mass, with increasing temperature of air along the gate the heat flux coming from rock mass decreases. The value of the heat flux depends on the temperature difference between air and ribs of the gate as well as on the duration of the period the gate was ventilated. The results summarized in Tables 1 and 3 show that along a substantial part of the length of the gate the former factor is decisive.

Only along the last 200 m section of the gate length the shorter period of ventilation prevails and causes some increase in heat flux coming from rock mass. The data in Tables 1 and 3 demonstrate clearly that the heat flux coming from rock mass is dependent on the temperature of rock. Assuming fresh air temperature at the start of the gate  $t_0 = 20^\circ\text{C}$ , this flux for  $t_{pg} = 40^\circ\text{C}$  is 65% higher in comparison with the case of  $t_{pg} = 35^\circ\text{C}$ , and if  $t_{pg} = 50^\circ\text{C}$ , it is 2.5 times higher. Similar relationships have been found as a result of calculations concerning the increase in air enthalpy along the entire length of the gate:  $\Delta I_{35} = 161.0$  kW,  $\Delta I_{40} = 207.4$  kW and  $\Delta I_{50} = 303.4$  kW.

For the variant of calculations with active technological sources of heat (Tables 2 and 4), heat flux from rock mass decreases steadily along the gate length. The presence of active technological heat sources as an additional source of heat and moisture causes greater increase in air temperature, which in turn results in lower values of difference between temperature of ribs and flowing air. In this case the previously occurring pattern is preserved, namely with increasing temperature of rock mass both heat flux coming from rock mass and stream of air enthalpy do increase. However, the proportions change:  $\Delta I_{35} = 474.9$  kW,  $\Delta I_{40} = 518.3$  kW,  $\Delta I_{50} = 610.5$  kW. In the variant with active technological sources of heat and moisture for the conditions assumed for the above presented example of calculations, a  $10^\circ\text{C}$  increase of temperature of rock mass causes the air enthalpy stream to be higher by about 90 kW.

For the assumed values of the parameters the presence of technological heat sources active along a mine working bring about the increase of enthalpy flux by 300 kW at the terminal cross section of the working. If the working is completed, i.e. no mining machinery is active, the increase of enthalpy is caused by heat of surrounding rock mass only.

The results of computer aided simulations are presented in graphical form in Figures 1, 2, 3 and 4. In these figures the dotted lines ‘dot-dot-dot-dot’ refer to rock mass temperature equal to  $35^\circ\text{C}$ , dashed lines: ‘dash-dash’ refer to rock mass temperature of  $40^\circ\text{C}$ , whereas the solid lines refer to temperature of rocks of  $50^\circ\text{C}$ . A  $10^\circ\text{C}$  increment in rock mass temperature causes increase in the air temperature gain by approximately  $5^\circ\text{C}$  (Fig. 1), regardless of the presence or lack of the technological sources of heat along the gate.

In the case of heat flux coming from rock mass its value depends on temperature of rock mass and the presence of technological heat sources (Fig. 2). If these sources are not active, the decrease in the value of this stream depends, but rather slightly, only on the temperature of rocks. For  $t_{pg} = 35^\circ\text{C}$  this decline is about 30%, for  $t_{pg} = 40^\circ\text{C}$  is about 26% and for  $t_{pg} = 50^\circ\text{C}$  it is 25%. With active technological heat sources the heat flux from rock mass decreases along the gate by about 69% for  $t_{pg} = 35^\circ\text{C}$ , by about 56% for  $t_{pg} = 40^\circ\text{C}$  and by about 46% for  $t_{pg} = 50^\circ\text{C}$ .

After analysis of Figure 3, which shows the change in stream of enthalpy of air, it has been decided to investigate how large is the ‘buffering effect of rock mass’ on the micro-climatic conditions along the gate with active technology heat sources.

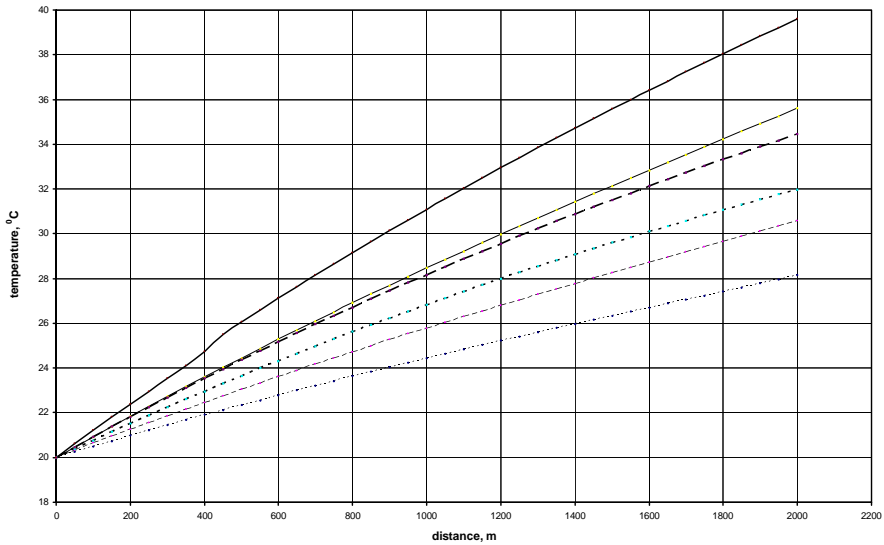


Fig. 1. Changes of temperature of air along a non-coal rocks surrounded mine working.

Explanation of the graphs:

- ..... -  $t_{pg} = 35^\circ\text{C}$  no technological sources;
- -  $t_{pg} = 50^\circ\text{C}$  no technological sources;
- -  $t_{pg} = 40^\circ\text{C}$  with technological sources;
- ..... -  $t_{pg} = 35^\circ\text{C}$  with technological sources;
- -  $t_{pg} = 50^\circ\text{C}$  with technological sources;
- -  $t_{pg} = 40^\circ\text{C}$  no technological sources;

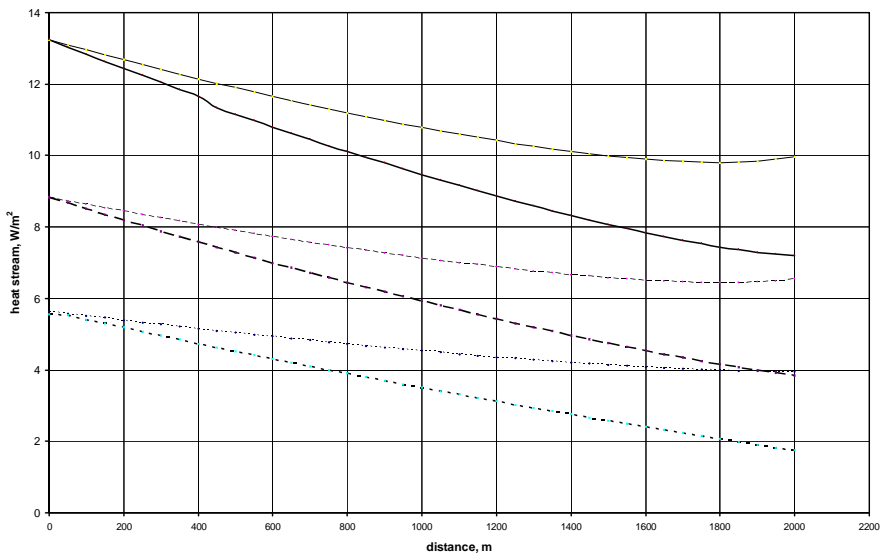


Fig. 2. The effect of temperature of rock mass on density of heat flux coming from the rock mass.

Explanation of the graphs:

- ..... -  $t_{pg} = 35^\circ\text{C}$  no technological sources;
- -  $t_{pg} = 50^\circ\text{C}$  no technological sources;
- -  $t_{pg} = 40^\circ\text{C}$  with technological sources;
- ..... -  $t_{pg} = 35^\circ\text{C}$  with technological sources;
- -  $t_{pg} = 50^\circ\text{C}$  with technological sources;
- -  $t_{pg} = 40^\circ\text{C}$  no technological sources;

Using the results presented in Tables 3 and 4, that part of air enthalpy flux which comes from technological heat sources was identified and separated. Figure 4 shows the distribution along the gate of the enthalpy flux coming from technological heat sources. It is apparent that the temperature of rock mass has virtually no effect on the technological part of air enthalpy flux. For the rock mass temperature equal to 35°C the technological part of enthalpy flux is about 25% of the total enthalpy, whereas for 40°C this share is 24% and for 50°C it is only 22%. Thus, the “buffering effect of the rock mass” on climate related parameters of air flowing along the working is negligible – the best part of the installed electrical power is used to perform useful work (to overcome intermolecular forces during extraction of coal, transport, etc.).

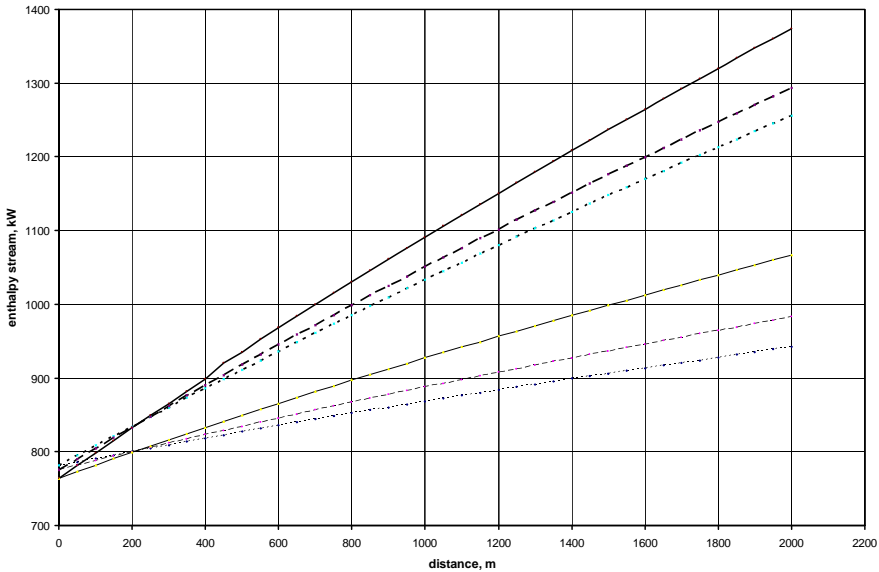


Fig. 3. Change of enthalpy of air flowing along a non-coal rock surrounded working.

Explanation of the graphs:

- ..... -  $t_{pg} = 35^\circ\text{C}$  no technological sources;
- -  $t_{pg} = 50^\circ\text{C}$  no technological sources;
- -  $t_{pg} = 40^\circ\text{C}$  with technological sources;
- ..... -  $t_{pg} = 35^\circ\text{C}$  with technological sources;
- -  $t_{pg} = 40^\circ\text{C}$  no technological sources;
- ..... -  $t_{pg} = 35^\circ\text{C}$  with technological sources;
- -  $t_{pg} = 50^\circ\text{C}$  with technological sources

### 3.2. The heat flux transferred from rock mass into gates surrounded by non-coal rocks

The effect of temperature of rock mass and of heat and moisture coming from technological sources on changes in flux of enthalpy of air flowing along a gate surrounded by non-coal rocks was studied. From these studies the following observations were derived:

- the presence of technological heat and moisture sources causes the increase of air temperature at the end of the gate by 4°C, regardless of the temperature of rock,
- the effect of temperature of rock mass on air temperature is significant, the increase of temperature of rocks by 10°C results in an increase of air temperature at the end of the

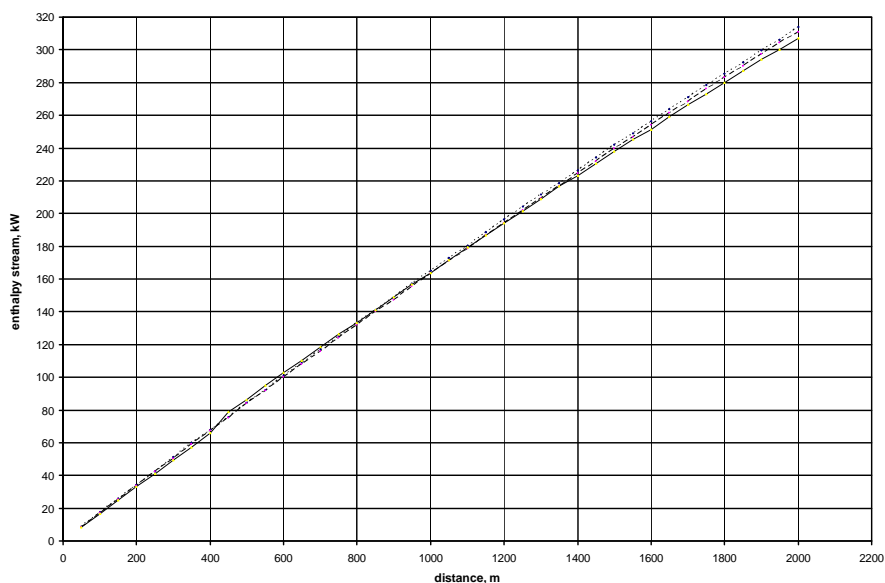


Fig. 4. Effect of temperature of rock mass on changes of enthalpy of air caused by technological heat sources.

Explanation of the graphs:

..... -  $t_{pg} = 35^\circ\text{C}$ ;

----- -  $t_{pg} = 40^\circ\text{C}$ ;

————— -  $t_{pg} = 50^\circ\text{C}$

- gate by  $5^\circ\text{C}$ , regardless of presence or lack of technological sources of heat, high increase in temperature of rocks causes the air temperature to be higher than in the case of a gate surrounded by rocks of lower temperature even with the presence of active and strong technological sources of heat (as is apparent from Figure 1),
- the increase in virgin rock mass temperature causes proportional increase of heat flux coming from rock mass – assuming that the temperature of fresh air at the beginning of the gate is  $20^\circ\text{C}$  – heat flux at  $T_{pg} = 40^\circ\text{C}$  is 65% higher than the flux for  $t_{pg} = 35^\circ\text{C}$  and for  $t_{pg} = 50^\circ\text{C}$  it is three times higher,
  - heat flux coming from rock mass depends not only on virgin temperature of rock mass itself but also on the presence of technological sources of heat and moisture – at low temperature of rock mass of the relative decline of that heat flux is significant when technological heat sources are active along the gate, with increasing temperature of rock mass this relative decline of heat flux from the rock mass is smaller,
  - the part of air enthalpy flux coming from the technological sources does not depend significantly on the virgin temperature of rock mass, ‘rock buffering effect’ on the climate parameters of air in the presence of active and powerful technical equipment and high temperature of rocks is negligible.

## 4. The effect of rock mass virgin temperature on the heat flux distribution along a coal working

In the case of a longwall gate driven in coal, in addition to heat sources that operate in the gates surrounded by non-coal rock (heat from rock mass, technological sources of heat) one have to also take into account the heat coming from the oxidation of coal.

In the scientific literature dealing with the topic, mainly published by Russian researchers (Szczerbań & Kremniew, 1959), it was assumed that the heat flux from coal oxidation can be quantified as the product of the exposed surface area of the coal walls (ribs, roof) of the gate and the unitary heat flux from coal oxidation. From the findings of Cygankiewicz J. (2012, 2012b), it has emerged that the heat of oxidation depends on the mass of coal undergoing oxidation. Since the rock mass around the gate is usually cracked, the mass of coal being oxidized depends on the extend of the fissures network within coal seam.

### 4.1. Determination of mass of coal undergoing oxidation

In order to determine the mass of coal undergoing oxidation one have to assess the extent of the cracks system within the rock mass around the gate. J. Drzewiecki and J. Smolka (1994) studied the fracturing of rock surrounding longwall gate. The authors assumed the following parameters as indicative of rock (coal) fracturing:

- equivalent surface area of cracks,  $S_o$ ,
- degree of fracturing of rocks  $K_s$ ,
- equivalent opening of cracks  $R_s$ ,

and then studied changes of these parameters along the distance from the gate ribs into the undisturbed rock-mass.

The results of this study are presented in Figure 5, which shows the effect of the distance from the ribs into the undisturbed rock mass on the extend and size of the fractured zone in the rock mass. Based on Figure 5 it can be assumed that the noticeable effect of rock fracturing extends for about 6 m, measured from ribs of the gate into the undisturbed rock mass. Therefore, in our reasoning such a zone was considered, limited by the assumed boundary between the cracked and the not disturbed areas. Cross-sectional surface of the area is in the shape of external semi-ellipse, with internal semi-ellipse excised, (Fig. 6), with outer ellipse's semi-axes  $a_1$  and  $b_1$ , and internal – ellipse's  $a_0$  and  $b_0$  respectively. Cross-sectional area of the area can thus be determined by the formula:

$$A_{el} = \frac{\pi \cdot a_1 \cdot b_1}{2} - \frac{\pi \cdot a_0 \cdot b_0}{2} = \frac{\pi}{2} (a_1 \cdot b_1 - a_0 \cdot b_0) \quad (18)$$

If such a zone is intersected by a seam of coal, the part of the surface area covered by coal can be calculated as the difference between the area from formula (18) and the surface area of the outer ellipse, less the surface area of a section of the inner ellipse. Since the surface area of an ellipse is defined by formula (Bronsztejn & Siemiendajew, 1970):

$$S = a \cdot b \cdot \arccos \frac{x}{a} - x \cdot y \quad (19)$$

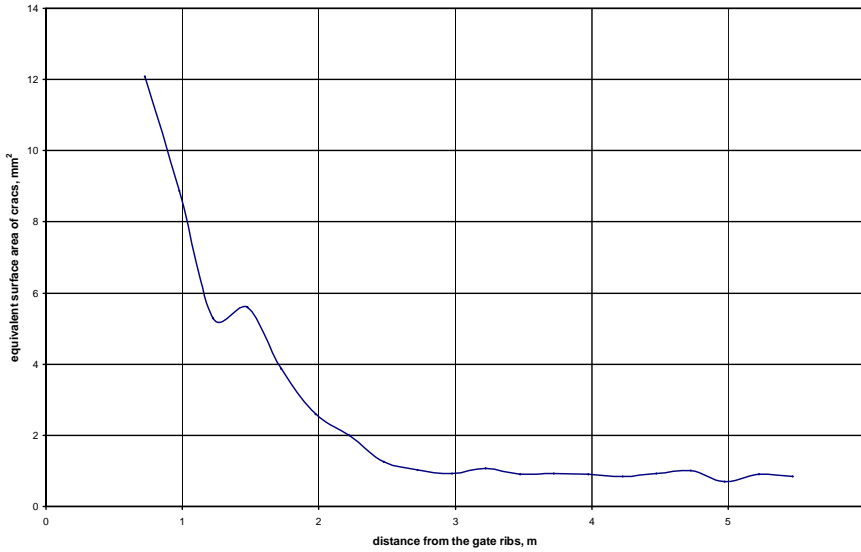


Fig. 5. Effect of distance from the gate ribs into undisturbed rock mass zone on the size of cracks, by J. Drzewiecki and J. Smolka (1994)

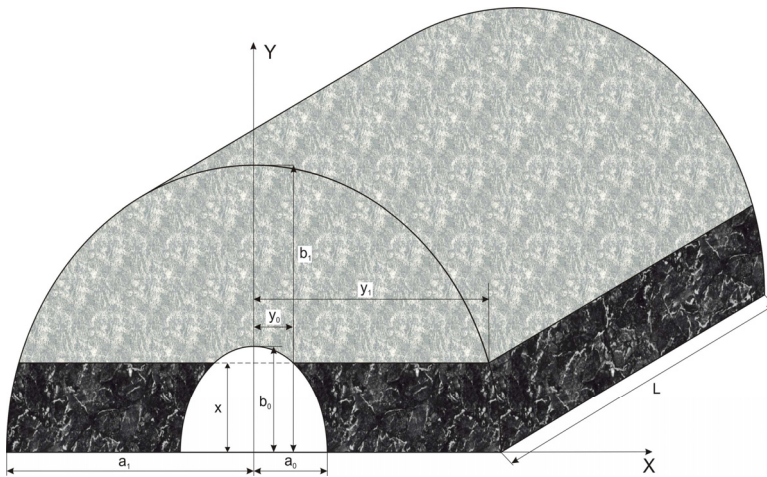


Fig. 6. A zone of fractured rock mass surrounding gate

where  $a$  and  $b$  are semi-axes of an ellipse,  $x$  and  $y$  are Cartesian coordinates, thus the surface area of the section of the outer ellipse is:

$$S_z = a_1 \cdot b_1 \cdot \arccos \frac{x}{a_1} - x \cdot y_1 \tag{20a}$$

And the surface area of the section of the inner ellipse is:

$$S_w = a_0 \cdot b_0 \cdot \arccos \frac{x}{a_0} - x \cdot y_0 \quad (20b)$$

Combining the relationships (18), (20a) and (20b), and multiplying the surface area by the length  $L$  of a section of the gate surrounded by the considered fractured zone one can calculate the volume of coal undergoing oxidation and obviously its mass by multiplying volume by coal density.

$$V = L \cdot \left[ \frac{\pi}{2} \cdot (a_1 \cdot b_1 - a_0 \cdot b_0) - a_1 \cdot b_1 \cdot \arccos \frac{x}{a_1} + a_0 \cdot b_0 \cdot \arccos \frac{x}{a_0} - x(y_1 - y_0) \right] \quad (21)$$

#### 4.2. The effect of temperature of rock mass and duration of ventilation period on heat flux resulting from oxidation of coal

The results of study by J. Cygankiewicz (2012, 2012b) indicate that the heat of oxidation of coal depends, among others, on the temperature of rock mass. This is illustrated in Table 5.

TABLE 5

The effect of temperature of rock mass on the oxidation heat of coal by J. Cygankiewicz (2012)

Nu.	Mine	Seam	Sponcom propensity group	Heat emitted from 1 kg of coal at temperature:		Temperature of rock-mass- $t_{pg}$ , °C	Ratio $Q_{(50)}/Q_{(t_{pg})}$
				50°C, J	Temperature, J		
1	2	3	4	5	6	7	8
1	Borynia	407/1	I	316	161	43	1.963
2	Borynia	405/1	I	299	152	42	1.967
3	Zofiówka	413	I	270	138	38	1.957
4	Zofiówka	502	I	241	123	43	1.959
5	Pniówek	364	I	287	146	40	1.966
6	Pniówek	403	I	276	141	42	1.957
7	Budryk	358	II	527	99	34	5.323
8	Bolesław Śmiały	325	II	445	84	32	5.298
9	Marcel	507	II	396	74	36	5.351
10	Sośnica	414/2	II	414	78	38	5.308
11	Budryk	364	II	333	62	35	5.371
12	Halemba	405	II	439	83	40	5.289
13	Murcki	364	III	1710	113	28	15.133
14	Jankowice	405/2	III	1548	102	34	15.176
15	Pokój	418	III	1746	115	40	15.183



1	2	3	4	5	6	7	8
16	Rydułtowy	620	III	1494	99	34	15.091
17	Anna	703	III	1512	100	35	15.120
18	Staszic	402	III	1710	113	41	15.133
19	Chwałowice	404	III	2510	207	25	12.126
20	Wieczorek	510	IV	2363	170	30	13.900
21	Wesoła	501	IV	3056	220	39	13.891
22	Ziemowit	206	IV	2774	200	29	13.870
23	Piast	206/1	IV	2594	187	28	13.872
24	Staszic	510	IV	2363	170	42	13.900
25	Bobrek	507	IV	2800	201	38	13.930
26	Ziemowit	209	V	3690	199	23	18.542
27	Centrum	503	V	6057	235	32	25.774
28	Sobieski	209	V	6648	258	30	25.767
29	Piast	209	V	6254	243	28	25.737
30	Jaworzno	207	V	8694	218	20	39.881

In this table values of the following parameters are given in appropriate columns: the name of the mine, the coal seam symbol, category of susceptibility to spontaneous ignition, heat emitted from 1 kg of coal during 2 hours test at 50°C, heat emitted during test at temperature equal to virgin temperature of rock mass at the site of sample collecting, the oxidation heats ratio of  $Q_{(50)}/Q_{(TPG)}$ . In all cases, the virgin temperature of rock mass at the site of sample collecting was lower than 50°C. From Table 5 it is also apparent that for coal classified to the first (lowest) group of susceptibility to spontaneous ignition the oxidation heat determined during test at 50°C is nearly two times greater than the heat of oxidation determined during tests at temperature equal to the virgin temperature of rock mass at the site of sample collecting. For the coal samples belonging to the second group of susceptibility to spontaneous ignition this ratio is about 5.3, whereas for the coal samples belonging to the third group of susceptibility to spontaneous combustion the ratio is 15, and for the coal samples classified to the fourth group of susceptibility to spontaneous combustion the ratio is about 13.9, and finally, for the coal samples classified to the fifth group of susceptibility to spontaneous combustion the ratio is the highest – it amount to 20 and more. Using the data in Table 5 the following linear dependencies of coal oxidation heat versus virgin temperature of rock mass were derived (using statistical methods):

- for the coal samples classified to the first group of propensity to spontaneous combustion:  $Q_I = 2.045 \cdot 10^{-3} \cdot t_{pg} - 0.06386$ , W/kg;  
(n.b. the relation is only valid for  $t_{pg}$  higher than 31.3°C)
- for the coal samples classified to the second group of propensity to spontaneous combustion:  $Q_{II} = 3.264 \cdot 10^{-3} \cdot t_{pg} - 0.1042$ , W/kg  
(n.b. the relation is only valid for  $t_{pg}$  higher than 32°C)
- for the coal samples classified to the third group of propensity to spontaneous combustion:  $Q_{III} = 0.01134 \cdot t_{pg} - 0.3457$ , W/kg;  
(n.b. the relation is only valid for  $t_{pg}$  higher than 30.6°C)
- for the coal samples classified to the fourth group of propensity to spontaneous combustion:  $Q_{IV} = 0.01736 \cdot t_{pg} - 0.5331$ , W/kg;  
(n.b. the relation is only valid for  $t_{pg}$  higher than 30.8°C)

- for the coal samples classified to the fifth group of propensity to spontaneous combustion:  
 $Q_V = 0.03345 t_{pg} - 0.8297$ , W/kg;  
 (n.b. the relation is only valid for  $t_{pg}$  higher than 24.9°C)

The listed above relations were derived on the basis of the experimental data. The validity of these expressions is limited, because they cannot be applied for the cases where the values of virgin temperature of rock mass is lower then the specific values determined for each of the five groups of coal susceptibility to spontaneous combustion. This limitation pertains especially for coals classified into the fifth (V) group of susceptibility to spontaneous combustion, whereas such coals can be encountered in many coal mines where climate related hazard is virtually nonexistent. During the preliminary statistical analysis of the data it has emerged that the best correlation can be achieved for linear regression, therefore such a regression was applied.

The correlation coefficient for the above relations is quite high, ranging from 0.86 (for  $Q_{III}$ ) to 0.93 (for  $Q_{II}$ ).

With regard to the scope of applicability of the above relations we assume they will be used only for the rocks of virgin temperature 35°C or higher.

Further analysis of the results of J. Cygankiewicz (2012a) indicates that the value of heat of oxidation of coal at the virgin temperature of rock-mass of about 35°C roughly corresponds to the value given by AN and OA Szerban Kremniew (1959). For the temperature of rock mass of about 40°C this value is two times higher, whereas for the temperature of 50°C it is four times higher. Effect of time lapse on the value of coal oxidation heat was determined by Cygankiewicz J. (2012b) based on the following drawing. Fig. 7.

Fig. 7 shows that while at the initial point heat of oxidation is very high its value rapidly decreases over time, after 50 days the heat of oxidation is 4.3% of the initial value and asymptotically, reaching a plateau after 1500 hours (62.5 days). By approximation it is assumed that after 250 days heat of oxidation is 2.6% of the original value.

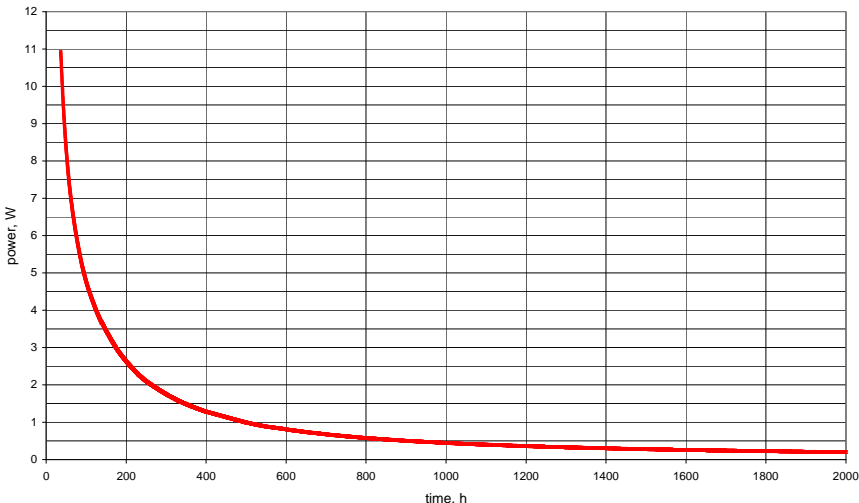


Fig. 7. Effect of time lapse on the value of oxidation heat of coal collected from Jaworzno mine, by J. Cygankiewicz (2012b)

In our further reasoning we assume that this relation is valid for all hard coals, notwithstanding their susceptibility to spontaneous combustion.

The data presented in Tables 6 and 7 show that the increase of virgin temperature of rock mass from 35°C to 40°C brings about a 5°C increase in temperature of air at the end of the working, whereas the increase of rock mass temperature from 40°C to 50°C causes a 10°C increase in air temperature. It can be said therefore that a 10°C increase in rock mass temperature brings about a 10°C increase in the temperature of air.

### 4.3. The heat of oxidation of coal along a longwall gate

In this computational example a longwall gate is considered,  $L=2000$  m long, of cross-sectional surface area  $A = 13.5 \text{ m}^2$ , velocity of air flowing along the gate is  $w = 1$  m/s. Along the gate a set of mining machines is installed of the total power  $N_m = 1$  MW. Three different temperatures of virgin temperature of rock mass surrounding the gate were assumed, namely:  $t_{pg1} = 50^\circ\text{C}$ ,  $t_{pg2} = 40^\circ\text{C}$ ,  $t_{pg3} = 35^\circ\text{C}$ . The length of the gate is divided into 40 segments, of length  $L = 50$  m each. It is assumed that the temperature of fresh air entering the gate intake cross section is  $t_0 = 20^\circ\text{C}$  and its relative humidity  $\varphi_0 = 72\%$ . It is also assumed that the thickness of a coal seam is 2.8 m, and that the coal was classified as belonging to the second group of susceptibility to spontaneous combustion. The geometrical dimensions of the gate road are as follows: width  $a = 4.8$  m, height  $h = 3.8$  m. Based on the reasoning presented in chapter 4.1 the volume of coal undergoing oxidation was determined. For the assumed values of the listed above parameters the quantities calculated according to formulas: (18), (20a), (20b) and (21) are as follows:

$$a_0 = 3.8 \text{ m}, b_0 = 2.4 \text{ m}, a_1 = 9.8 \text{ m}, b_1 = 8.4 \text{ m}, x = 2.8 \text{ m}, y_0 = 1.5 \text{ m}, y_1 = 7.5 \text{ m}.$$

Assuming that the extend of the fractured area reaches 6 m in depth, measuring from the surface of the gate ribs, the estimated value of cross-sectional surface area occupied by the coal is  $33.0974 \text{ m}^2$ . By multiplying the resulting value by the length of the gate section the volume of coal oxidation zone in this section is  $1654.87 \text{ m}^3$ , therefore its mass is 2 482 310 kg. Because the coal is classified into the second category of susceptibility to spontaneous ignition, therefore the heat of coal oxidation at 50°C is 0.05900 W / kg, at 40°C it is 0.02636 W / kg and at the temperature of 35°C it is 0.01004 kW. By multiplying these values by the mass of coal undergoing oxidation the value can be calculated of the heat produced from coal oxidation process at the initial moment of ventilation of the gate. This value is very high – for the rock mass temperature equal to 50°C it amounts to 146.456 kW, for the temperature of 40°C it is 65.434 kW, whereas for temperature of 35°C it is 24.922 kW. Due to the fact that the duration of ventilation period of different sections of the gate are different, the values of heat fluxes created due to oxidation of coal also differ. Using the relationship presented in Figure 7 the changes in coal oxidation heat along the exemplary longwall gate were estimated, basing on the assumption that tendency of these changes is the same as in the case of coal from the mine Jaworzno.

### 4.4. Computer aided simulations

As in Chapter 3, calculations for three variant were carried out (for the following temperatures of rock mass: 35°C, 40°C and 50°C) in order to asses the values of heat flux transferred from rock mass into the air stream carried along a longwall gate. The gate was divided into a number of segments, 50 m in length each. Air temperature –  $t_w$ , degree of moisture- $X$  and enthalpy of

air stream at the beginning and at the end of each segment were calculated, taking into account technological heat sources. The results of calculations are presented in Table 6. Data in Table 7 summarizes the calculated changes in heat flux distribution along the gate, with the coal oxidation part of the heat flux singled out in a separate column.

In the case of a gate surrounded by coal the value of stream of air enthalpy increases with increasing temperature of rock mass but that increase is larger than in the case of gate (working) surrounded by non-coal rocks. It can be attributed to the presence of an additional source of heat due to oxidation of coal. If the temperature of surrounding rocks mass is  $35^{\circ}\text{C}$   $\Delta I_{30} = 502$  kW, i.e. 341 kW more than in a non-coal rock surrounded gallery, for  $t_{pg} = 40^{\circ}\text{C}$   $\Delta I_{40} = 591$  kW, 383.6 kW more than in a non-coal rock gate. If, however, the  $t_{pg} = 50^{\circ}\text{C}$   $\Delta I_{50} = 768$  kW, an increase of more than 464.6 kW than in the case of non-coal rock gallery. The differences in enthalpy increase obviously are associated with heat of oxidation increasing with rock mass temperature.

The data from Table 6 suggest that the air stream temperature along a longwall gate is growing much more steeper than in the case of a gallery surrounded by non-coal rocks. For the temperature of rock mass of  $35^{\circ}\text{C}$  the temperature rise is about 13% higher, and is 28% if temperature of rock mass is  $40^{\circ}\text{C}$ , and for  $t_{pg} = 50^{\circ}\text{C}$  the increase in air temperature is about 44% higher in comparison with the increase in a non-coal rock surrounded gallery. For the variant with the rock mass temperature of  $30^{\circ}\text{C}$  air temperature can be even higher than the temperature of surrounding rocks. This is a result of active technological sources of heat and ongoing process of coal oxidation. The rise of rock mass temperature from  $35^{\circ}\text{C}$  to  $40^{\circ}\text{C}$  produces air temperature increase by about  $5^{\circ}\text{C}$ . However, the rise of rock mass temperature from  $40^{\circ}\text{C}$  to  $50^{\circ}\text{C}$  involves air temperature increasing by about  $15^{\circ}$  in comparison with the case of rock mass temperature equal to  $35^{\circ}\text{C}$ . If an intensive ventilation scheme is applied as the only heat hazard prevention means (with no air conditioning) the temperature of air at the end of the gate (at the junction with the longwall) is close to the temperature of rock mass.

As in the previous case of a gallery surrounded by non-coal rocks the heat flux transferred from rock-mass into the air stream flowing along a gate depends on temperature of rock mass and temperature of air. Also as in the previous case, the value of heat flux decreases along the length of the gate, but, due to coal oxidation heat it is still higher than the corresponding heat flux in a non-coal rock surrounded gallery. In the table 7 the distribution of heat flux from coal oxidation is presented along with heat flux from surrounding rocks. Since, as it was demonstrated by Cygankiewicz J. (2012b), this flux is time depending, its value increases when approaching the end point – the intersection of the gate with longwall. Also, this flux is heavily dependent on the temperature of surrounding rocks. A  $10^{\circ}\text{C}$  increase in the temperature of rocks will more than double the heat flux from coal oxidation.

The results of computer aided simulations are presented in graphs. Figure 8 shows the effect of temperature of rock mass on temperature of air stream along a gate with extracted coal haulage. The dotted line ‘dot-dot-dot’ refers to the case of temperature of rock mass equal to  $35^{\circ}\text{C}$ , the line ‘dash-dash’ refers to temperature of  $40^{\circ}\text{C}$  and the solid line to temperature of  $50^{\circ}\text{C}$ . Figure 9 illustrates the effect of virgin temperature of rock mass on the flux of heat coming from rock mass, with the part of the heat flux deriving from oxidation of coal marked separately. While the total heat flux from rock mass decreases with the increasing distance from the beginning of the gate (due to decreasing of temperature difference between air and ribs), the coal oxidation heat flux is increasing steadily. Figure 10 shows the change in the enthalpy of air flowing along the gate is depending on temperature of surrounding rocks. Assuming as a criterion the obligation required by Polish occupational regulations to maintain in mines temperature of air below  $28^{\circ}\text{C}$

TABLE 6

The effect of rock mass temperature on thermal parameters of air along a longwall gate with extracted coal haulage

s, m	$t_{pg} = 35^{\circ}\text{C}$			$t_{pg} = 40^{\circ}\text{C}$			$t_{pg} = 50^{\circ}\text{C}$		
	$t_w, ^{\circ}\text{C}$	X kg vapor/kg dry air	I, kW	$t_w, ^{\circ}\text{C}$	X kg vapor/kg dry air	I, kW	$t_w, ^{\circ}\text{C}$	X kg vapor/kg dry air	I, kW
0	20.00	0.00975	787	20.00	0.00948	775	20.00	0.00922	764
50	20.35	0.00990	800	20.56	0.00962	792	20.84	0.00937	785
100	20.69	0.01004	813	21.12	0.00977	808	21.67	0.00951	807
150	21.03	0.01018	825	21.67	0.00991	824	22.49	0.00965	828
200	21.36	0.01033	838	22.21	0.01005	841	23.31	0.00980	849
250	21.69	0.01047	850	22.75	0.01020	857	24.12	0.00994	870
300	22.02	0.01062	862	23.28	0.01034	873	24.92	0.01008	890
350	22.34	0.01076	874	23.81	0.01049	889	25.71	0.01022	911
400	22.66	0.01091	887	24.33	0.01063	904	26.50	0.01037	932
450	22.97	0.01105	899	24.84	0.01077	920	27.28	0.01051	952
500	23.28	0.01120	911	25.35	0.01092	936	28.05	0.01063	971
550	23.59	0.01134	923	25.85	0.01106	951	28.81	0.01080	992
600	23.89	0.01149	933	26.35	0.01121	966	29.57	0.01094	1013
650	24.19	0.01163	947	26.84	0.01135	982	30.32	0.01108	1033
700	24.49	0.01178	958	27.33	0.01149	997	31.06	0.01123	1052
750	24.78	0.01192	970	27.81	0.01164	1012	31.80	0.01137	1072
800	25.07	0.01207	982	28.29	0.01178	1027	32.53	0.01151	1092
850	25.35	0.01221	993	28.76	0.01193	1042	33.25	0.01165	1111
900	25.63	0.01235	1005	29.23	0.01207	1057	33.96	0.01180	1130
950	25.91	0.01250	1016	29.69	0.01221	1072	34.67	0.01194	1149
1000	26.18	0.01264	1028	30.15	0.01236	1087	35.37	0.01208	1169
1050	26.45	0.01279	1039	30.60	0.01250	1101	36.06	0.01223	1187
1100	26.72	0.01293	1050	31.05	0.01264	1116	36.75	0.01237	1206
1150	26.98	0.01308	1062	31.49	0.01279	1130	37.43	0.01251	1225
1200	27.24	0.01322	1073	31.92	0.01293	1144	38.10	0.01266	1244
1250	27.49	0.01337	1084	32.35	0.01308	1159	38.76	0.01280	1263
1300	27.74	0.01351	1095	32.77	0.01322	1173	39.42	0.01294	1280
1350	27.99	0.01366	1106	33.19	0.01336	1187	40.07	0.01309	1299
1400	28.23	0.01380	1117	33.60	0.01351	1201	40.71	0.01323	1317
1450	28.47	0.01395	1127	34.01	0.01365	1215	41.35	0.01337	1335
1500	28.71	0.01409	1138	34.41	0.01380	1228	41.98	0.01351	1353
1550	28.94	0.01423	1149	34.81	0.01394	1242	42.60	0.01366	1370
1600	29.17	0.01438	1160	35.20	0.01408	1256	43.21	0.01378	1387
1650	29.39	0.01452	1170	35.59	0.01423	1269	43.82	0.01394	1405
1700	29.61	0.01467	1181	35.97	0.01437	1282	44.42	0.01409	1423
1750	29.83	0.01481	1191	36.35	0.01452	1296	45.01	0.01423	1440
1800	30.04	0.01496	1201	36.72	0.01466	1309	45.60	0.01437	1457
1850	30.25	0.01510	1212	37.09	0.01480	1322	46.18	0.01452	1474
1900	30.45	0.01525	1222	37.45	0.01495	1335	46.75	0.01466	1491
1950	30.65	0.01539	1232	37.81	0.01509	1348	47.31	0.01480	1508
2000	30.85	0.01554	1242	38.16	0.01523	1361	47.86	0.01494	1524

The effect of rock mass temperature on heat flux transferred from the rock mass into air stream flowing along a gate with coal haulage

s, m	$t_{pg} = 35^{\circ}\text{C}$			$t_{pg} = 40^{\circ}\text{C}$			$t_{pg} = 50^{\circ}\text{C}$		
	$t_w, ^{\circ}\text{C}$	$Q_g, \text{W}$	incl. $Q_{\text{CO}_2}, \text{W}$	$t_w, ^{\circ}\text{C}$	$Q_g, \text{W}$	incl. $Q_{\text{CO}_2}, \text{W}$	$t_w, ^{\circ}\text{C}$	$Q_g, \text{W}$	incl. $Q_{\text{CO}_2}, \text{W}$
0	20.00	5013	648	20.00	7522	1701	20.00	12537	3808
50	20.43	4921	659	20.57	7414	1729	20.85	12398	3870
100	20.85	4833	669	21.13	7306	1756	21.70	12255	3932
150	21.27	4740	679	21.69	7200	1785	22.54	12117	3995
200	21.68	4654	691	22.24	7095	1812	23.37	11978	4057
250	22.09	4565	701	22.79	6988	1840	24.19	11843	4119
300	22.49	4477	711	23.33	6885	1868	25.00	11708	4181
350	22.89	4390	723	23.86	6786	1896	25.81	11570	4244
400	23.28	4306	733	24.39	6681	1923	26.61	11434	4305
450	23.67	4217	743	24.91	6583	1952	27.40	11300	4368
500	24.05	4134	754	25.43	6479	1979	28.18	11171	4431
550	24.43	4051	765	25.94	6380	2007	28.96	11036	4493
600	24.80	3970	775	26.44	6281	2035	29.73	10901	4555
650	25.17	3887	786	26.94	6191	2073	30.49	10770	4617
700	25.53	3808	797	27.43	6085	2090	31.24	10644	4680
750	25.89	3724	807	27.92	5987	2119	31.99	10508	4741
800	26.24	3647	817	28.40	5891	2146	32.73	10379	4804
850	26.59	3568	828	28.88	5796	2174	33.46	10252	4866
900	26.93	3489	839	29.35	5700	2201	34.18	10122	4929
950	27.27	3409	849	29.82	5602	2230	34.90	9994	4990
1000	27.61	3329	860	30.28	5506	2257	35.61	9865	5053
1050	27.94	3254	871	30.74	5411	2285	36.31	9738	5115
1100	28.27	3174	881	31.19	5316	2313	37.01	9607	5177
1150	28.59	3099	892	31.63	5225	2341	37.70	9476	5239
1200	28.91	3023	902	32.07	5129	2368	38.38	9351	5302
1250	29.22	2948	913	32.50	5039	2397	39.05	9220	5364
1300	29.53	2871	923	32.93	4947	2424	39.72	9093	5426
1350	29.84	2796	934	33.35	4852	2452	40.38	8962	5488
1400	30.14	2721	945	33.77	4761	2480	41.03	8833	5551
1450	30.44	2645	955	34.18	4666	2508	41.67	8702	5613
1500	30.73	2574	966	34.59	4570	2535	42.31	8567	5675
1550	31.02	2498	976	34.99	4480	2564	42.94	8437	5738
1600	31.31	2420	988	35.39	4384	2591	43.56	8302	5800
1650	31.59	2348	998	35.78	4289	2619	44.17	8167	5862
1700	31.87	2267	1008	36.17	4188	2646	44.78	8028	5924
1750	32.14	2195	1018	36.55	4094	2675	45.38	7886	5987
1800	32.41	2117	1030	36.93	3990	2702	45.97	7743	6049
1850	32.67	2041	1040	37.30	3891	2730	46.55	7596	6111
1900	32.93	1965	1050	37.66	3792	2758	47.12	7445	6173
1950	33.18	1890	1061	38.02	3684	2786	47.69	7285	6235
2000	33.48	1786	1072	38.43	3547	2813	48.31	6929	6297

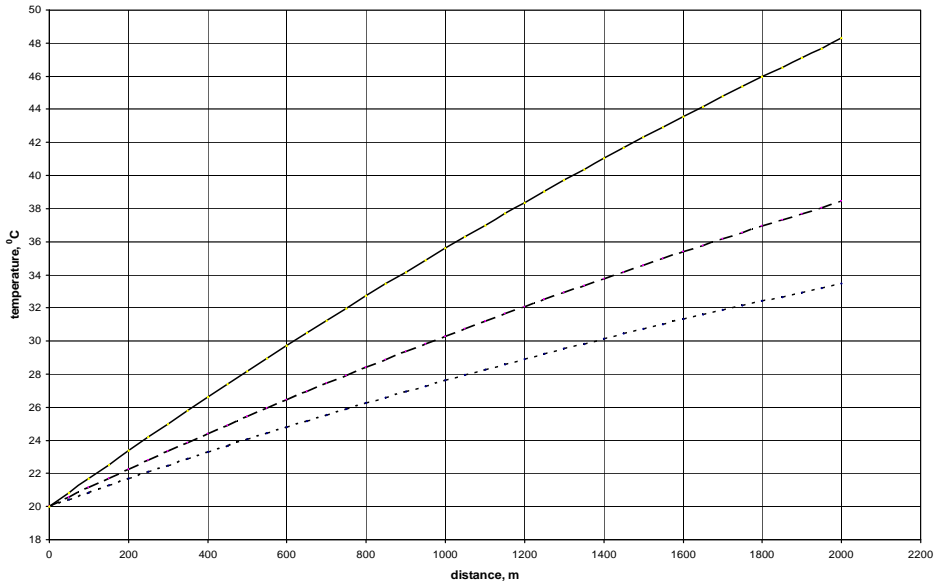


Fig. 8. The effect of rock mass temperature on temperature of air along the longwall gate with coal hauling.

Explanation of the graphs:

..... -  $t_{pg} = 35^\circ\text{C}$ ;      - - - - -  $t_{pg} = 40^\circ\text{C}$ ;      ———  $t_{pg} = 50^\circ\text{C}$

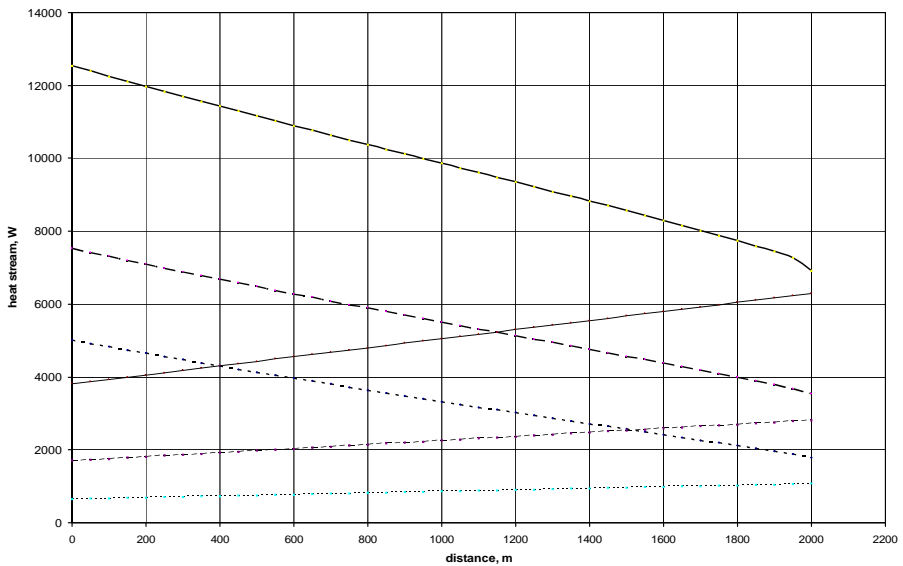


Fig. 9. The effect of virgin temperature of rock mass on heat flux coming from the rock mass.

Explanation of the graphs:

..... -  $Q_g(35^\circ\text{C})$ ;      - - - - -  $Q_g(40^\circ\text{C})$ ;      ———  $Q_g(50^\circ\text{C})$ ;  
 ..... -  $Q_{CO_2}(35^\circ\text{C})$ ;      - - - - -  $Q_{CO_2}(40^\circ\text{C})$ ;      ———  $Q_{CO_2}(50^\circ\text{C})$ ;





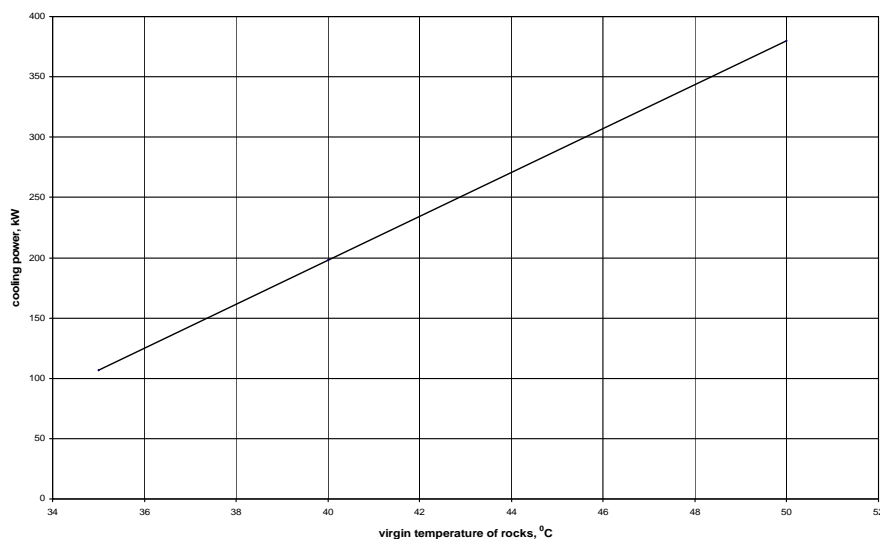


Fig. 11. The effect of rock mass temperature on the capacity of cooling system required for a gate 2000 m in length

greater than in the case of non-coal rock surrounded workings, due to heat of oxidation of coal. The research Cygankiewicz J. (2012b) showed that the oxidation heat is strongly dependent on the temperature of rocks.

A series of variant climatic parameters prognostic calculations were carried out in order to assess the merits of the presented new approach to the problem of impact high-temperature rock mass having on micro-climate related occupational conditions in gates surrounded by coal in comparison with the former approach (by Szczerbanin & Kremniew, 1959) where a constant value of heat of coal oxidation was assumed. In three instances of prognostic calculations a constant value of coal oxidation heat equal to  $7.56 \text{ W/m}^2$  was assumed. The next three prognoses were carried out with assumption that coal oxidation heat is dependent on the duration of the ventilation period of a gate and the temperature of rocks surrounding the gate. The results of calculations are presented in graphical form in Fig. 12. Dotted lines: 'dot-dot-dot' refer to  $t_{pg} = 35^\circ$ , dashed lines: 'dash-dash' refer to  $t_{pg} = 40^\circ$  and solid lines represent the results of calculations for  $t_{pg} = 50^\circ$ . Bold lines represent heat of oxidation determined on the basis of the results of Cygankiewicz J. (2012, 2012b), whereas thin lines pertain to the values calculated according to the approach by A.N. Szczerbanin and O.A. Kremniewa (1959).

For the assumed value of virgin rock mass temperature of  $35^\circ\text{C}$  and for constant value of coal oxidation heat the calculated value of air temperature at the end the gate is  $0.70^\circ\text{C}$  higher than the temperature calculated for the variant with variable coal oxidation heat value. For virgin rock mass temperature equal to  $40^\circ\text{C}$  though, temperature of air at the end of the gate for the variant with variable coal oxidation heat is about  $1.20^\circ\text{C}$  higher than for the constant coal oxidation heat. Finally, in the case of virgin temperature of rock mass of  $50^\circ\text{C}$ , the temperature of air at the end of the gate, calculated for the case of variable coal oxidation heat is  $5.60^\circ\text{C}$  higher than the temperature calculated for the constant value of the oxidation heat.

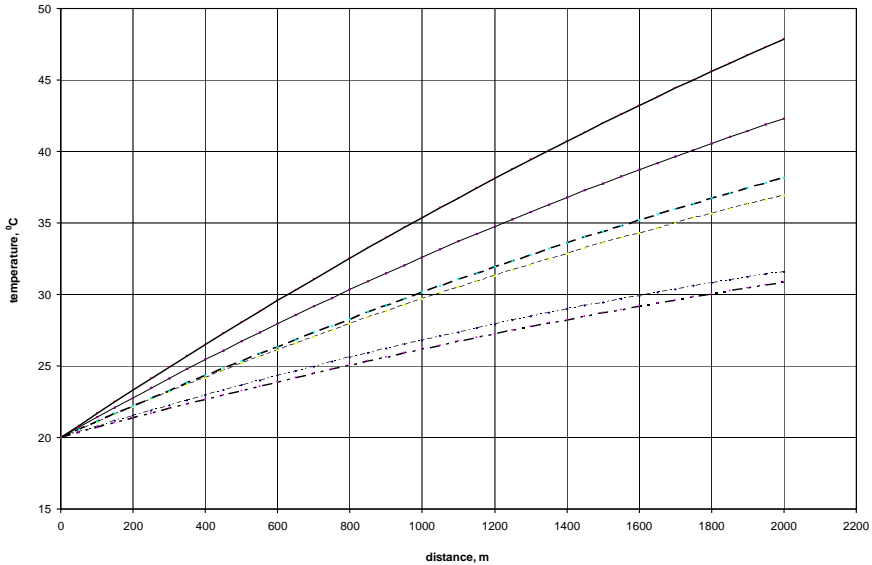


Fig. 12. Comparison of results of air temperature prognoses with assumption of constant and variable coal oxidation heat.

Explanation of the graphs:  
 ..... -  $t_{pg} = 35^\circ\text{C}$ ;      - - - - -  $t_{pg} = 40^\circ\text{C}$ ;      ———— -  $t_{pg} = 50^\circ\text{C}$   
 bold lines pertain to the case of variable value of coal oxidation heat,  
 in other graphs that value is assumed as a constant.

## 5. Conclusions

The rise of temperature of rocks surrounding underground mine workings causes deterioration of the micro-climate related occupational conditions there, regardless of the kind of surrounding rock (non-coal rocks, coal).

With regard to the studied case of a typical 2000 m working surrounded by non-coal rock the following conclusions can be drawn:

- External (technological) heat and moisture sources acting along a working cause air temperature rising by about 4°C.
- Temperature of rocks surrounding a gate has significant impact on air temperature, a rock mass temperature rise of about 10°C results in an increase of air temperature at the end of the working by 5°C, regardless of the presence or not of external (technological) heat and moisture sources.
- With increasing temperature of rock mass the heat flux from rock mass increases in proportion to the growth of rock mass temperature, for the initial temperature 20°C of air stream at the intake and virgin temperature of rocks of 40°C the heat flux is 65% higher than the heat flux at temperature of rocks = 35°, whereas the heat flux for 50°C is about 2.5 times higher.

- The value of heat flux coming from the surrounding rocks depends not only on the temperature of rocks but also on the presence of external (technological) sources of heat and moisture. At lower temperatures of rock mass and with active technological sources of heat and moisture the relative decline of the said heat flux is significant, whereas with increasing temperature of rock mass the relative decrease in heat flux coming from the rock mass is smaller.
- The part of air enthalpy, caused by technological sources, does not depend significantly on the temperature of rock mass, thus the expected “buffering effect of rock mass” on the micro-climate parameters in the case of active high power technological heat and moisture sources and high temperature of rock mass is negligible.

Similar conclusions pertain also to the case of a typical longwall gate surrounded by coal, but the influence of rock mass temperature on air temperature there is stronger, namely:

- A 10°C rise in rock mass temperature results in an increase in air temperature at the end of a gate by about  $7 \div 10^\circ\text{C}$ . In some cases, the said temperature of air can be even higher than the temperature of surrounding rocks.
- An increase of temperature of air along a coal surrounded gate is higher than in the case of a non-coal rocks surrounded working, it is so due to additional heat source – oxidation of coal.
- With regard to non-coal rocks surrounded workings the effect of fracturing of rock mass on temperature of air flowing along that working is negligible, while in the case of coal workings this impact is much more significant. For rock mass temperatures higher than 35°C the calculations of the value of heat flux from coal oxidation according to the approach by Szczerban and Kremniew (1959) yield too low results, so the approach of Cygankiewicz J. (2012a, 2012b) should be adopted, taking into account the temperature and time lapse dependency of coal oxidation flux.

## References

- Bronsztejn I.N., Siemiendajew K.A., 1970. *Matematyka. Poradnik Encyklopedyczny*. PWN, Warszawa.
- Břimek Z., Knechtel J., 2008. *Nowe spojrzenie na zwalczanie zagrożenia klimatycznego w oddziałach wydobywczych o skrajnie trudnych warunkach geotermicznych i dużej koncentracji wydobywania*. Materiały konferencyjne międzynarodowej konferencji: „Ventilation, Degassing and Air Conditioning of Coal Mines, Szpetna – Ostravice, 16÷17.09.2008.
- Cygankiewicz J. 2012a. *Nowe kryteria klasyfikacji skłonności węgla do samozapalenia*. Monografia: zwalczanie zagrożeń aerologicznych w kopalniach, praca zbiorowa pod redakcją S. Pruska, J. Knechtela i B. Madejki-Strumińskiej, GIG, Katowice.
- Cygankiewicz J. 2012b. *Kalorymetryczna metoda oznaczania skłonności węgla do samozapalenia w warunkach zbliżonych do warunków kopalnianych*, praca statutowa GIG o symbolu 1111 0222-110, Katowice.
- Drzewiecki J., Smółka J., 1994. *Przodki ścianowe o wysokiej koncentracji produkcji*. Rozdział III. Kompleksowe badania zjawisk zachodzących w górotworze. Część 3. Pomiary in situ nieciągłości zaistniałych w górnictwie na skutek szybko przemieszczającego się frontu ściany. Wyniki prac badawczo-rozwojowych realizowanych w ramach dotowanego przez KBN projektu celowego nr 231/CS6-9/92 pt.: Wysoko wydajny kompleks ścianowy i nowa technologia wydobycia węgla w KWK „Staszic”, Wyd. Pol. Śl., Katowice-Gliwice.
- Holek S. 1979. *Stanowisko badawcze do wyznaczania współczynników dotyczących ruchu ciepła i wilgoci w skałach*. Dokumentacja prac GIG o symbolu 01.4.05.02/16 2, Katowice.

- Holek S. 1982. *Badania nad zjawiskiem ruchu wilgoci i ciepła w górotworze dla ustalenia modelu tego zjawiska*. Dokumentacja prac GIG o symbolu MR.I.26.5.02/N02/82/B1, Katowice.
- Holek S., 1990. *Opracowanie potencjału ruchu wilgoci i opartych na nim metod prognozowania mikroklimatu wyrobisk*. Prace GIG, seria dodatkowa, Katowice.
- Knechtel J., 1998a. *Zagrożenie klimatyczne w polskich kopalniach węgla*. Prace Naukowe GIG, Komunikat nr 835, Katowice.
- Knechtel J., 1998b. *The Influence of Thermal Insulation of Walls of Workings on Air Temperature*, Arch. Min. Sci., Vol. 43, No 4, Kraków.
- Knechtel J., Gapiński D., 2005, *Zaktualizowane mapy izolinii temperatury pierwotnej skal kopalń Górnośląskiego Zagłębia Węglowego (GZW)*, Katowice, Główny Instytut Górnictwa.
- Knechtel J., 2009. *Wpływ lokalnych źródeł ciepła na mikroklimat w wysokowydajnych ścianach eksploatowanych podziemowo*. Praca statutowa GIG o symbolu: I.1.18/1101 1899-112, Katowice.
- Nikitienko N.I., 1971 *Issledowanije niestacionarnych processow tieplo- i masso-obmiena mietodom sietok*, Naukowa Dumka, Kijów.
- Sidiropoulos E., Tzimopoulos, 1983. *Sensitivity analysis of a coupled heat and mass transfer model in unsaturated porous media*. Journal of Hydrology, Vol. 64, p. 281-298.
- Szczerbań A.N., Kremniew O.A. 1959. *Naucznyje asnowy rasczota i reguliowanija tiepłowego režima głębokich szacht*. UAN, Kijów.

Received: 06 May 2013